

<https://doi.org/10.1038/s43247-024-01333-7>

# Restricted plant diversity limits carbon recapture after wildfire in warming boreal forests

Check for updates

Johan A. Eckdahl<sup>1,2</sup> , Jeppe A. Kristensen<sup>3,4</sup> & Daniel B. Metcalfe<sup>2</sup>

Incomplete wildfire combustion in boreal forests leaves behind legacy plant-soil feedbacks known to restrict plant biodiversity. These restrictions can inhibit carbon recapture after fire by limiting ecosystem transition to vegetation growth patterns that are capable of offsetting warmth-enhanced soil decomposition under climate change. Here, we field-surveyed plant regrowth conditions 2 years after 49 separate, naturally-occurring wildfires spanning the near-entire climatic range of boreal Fennoscandia in order to determine the local to regional scale drivers of early vegetation recovery. Minimal conifer reestablishment was found across a broad range of fire severities, though residual organic soil and plant structure was associated with restricted growth of a variety of more warmth-adapted vegetation, such as broadleaf trees. This dual regeneration limitation coincided with greater concentrations of bacterial decomposers in the soil under increased mean annual temperature, potentially enhancing soil carbon release. These results suggest that large portions of the boreal region are currently at risk of extending postfire periods of net emissions of carbon to the atmosphere under limitations in plant biodiversity generated by wildfire and a changing climate.

The boreal region is undergoing a transition towards broadleaf overstory dominance, a shift anticipated to be accelerated by longer and warmer growing seasons under continued climatic change<sup>1,2</sup>. The pace of this transition is currently limited by plant-soil feedbacks regulated by occupant coniferous overstory<sup>3</sup>. For example, thick, nutrient-poor organic soil layers and symbiosis with ectomycorrhizal fungi restrict overall plant biodiversity and promote establishment and growth of conifer seedlings over broad-leaved tree species<sup>4–9</sup>. High-severity wildfire can dismantle these limitations through near-complete removal of resident vegetation and organic soil layers, thereby creating favorable conditions for broadleaf tree germination and growth<sup>10,11</sup>. The extent of shifts in overstory dominance after fire then appears to be largely determined by the amount of on- and off-site provisioning of broadleaf generative material, such as seed and budding sources, which in turn is influenced by their landscape abundance in response to ongoing climatic change<sup>12,13</sup>. Vigorous recruitment of broadleaf trees after conifer forest wildfire can rapidly sequester carbon (C), reaching a greater total amount of C than that held in previous conifer forest structure, providing a net sink of greenhouse gasses from the atmosphere over the disturbance cycle<sup>13,14</sup>.

Under the recent decades of climatic instability, circumpolar reductions in boreal conifer recovery capacity are also being observed even under lower-severity wildfire<sup>1,12,15,16</sup>. However, more information is needed regarding the mechanisms and extent by which biotically-derived material left behind after fire can continue to resist alternate growth of both overstory and understorey vegetation. Conversely, heat-altered organic soil material can serve as a steady source of nutrients under warmth-enhanced soil decomposition, supporting more temperate, resource-demanding plant species<sup>17</sup>. Although, limited propagule inputs of novel species to burn scars due to slowly-migrating landscape vegetation cover, and their interaction with remaining plant-soil feedbacks (such as thick organic soil layers and ecto- and ericoid mycorrhizas), could limit the effect of enhanced growing conditions on C recapture in the early postfire environment<sup>18–21</sup>. In light of these combined challenges to regeneration under climate change, we propose that intermediate ranges of fire severity in warming boreal forests can both restrict recovery of occupant overstory species by reducing their reproductive capabilities while failing to completely remove the plant-soil feedbacks capable of strengthening biodiversity constraints on overall vegetation recovery. A dual limitation of occupant and novel species

<sup>1</sup>Department of Physical Geography and Ecosystem Science, Lund University, Lund, Sweden. <sup>2</sup>Department of Ecology and Environmental Science, Umeå University, Umeå, Sweden. <sup>3</sup>Environmental Change Institute, School of Geography and the Environment, University of Oxford, Oxford, UK. <sup>4</sup>Department of Biology, Aarhus University, Aarhus, Denmark. e-mail: [Johan.Eckdahl@nateko.lu.se](mailto:Johan.Eckdahl@nateko.lu.se)

regrowth under increased decomposition presents a risk for enhancing the severity and duration of net forest C emissions occurring during the years following the initial period of wildfire combustion<sup>22</sup>. Lengthened delays in the transition of boreal forests to C sinks after wildfire can leave a greater portion of their landscape in relatively low C states at any given time, consequently shifting the C balance further from the land to the atmosphere in the coming century. Although, the environmental factors regulating these dynamics remain largely unknown, limiting predictions of boreal forest C cycling under a changing climate.

This study surveyed the plant reestablishment stage within 2 years following fire across 49 separate conifer forest wildfires spanning a 7.3 °C mean annual temperature (MAT) range in boreal Fennoscandia (Fig. 1a). The aim was to investigate patterns of ecosystem reorganization after burning to determine how C recapture is controlled by the interactions of plant regrowth with residual ecosystem vegetation, microbial communities, soil structure and climate (Fig. 2). It was hypothesized that a broad range of fire severity (determined by alteration of organic soil material and overstory mortality) impaired the early recovery capacity of previous vegetation while restricting plant community turnover. Resulting stagnation in primary production capacity was expected to coincide with a MAT-enhanced shift in soil communities towards bacterial decomposers. It was anticipated that these complex interactions would emerge as low levels of plant biodiversity that constrain the ability of boreal ecosystems to recapture C under increased warmth, likely establishing longer-term forest recovery trajectories that limit landscape C storage over the coming decades of climatic change.

## Results and discussion

Across the 49 sampled fire plots, a broad range of residual organic layer thickness (ResOL, 2.5 to 17.1 cm, mean 7.0 cm), surviving conifer basal area (LiveConifer 0.0 to 47.5 m<sup>2</sup> ha<sup>-1</sup>, mean 14.4 m<sup>2</sup> ha<sup>-1</sup>) and estimated depth of

organic layer burn (BurnDepth, mean 4.6 cm, standard deviation 4.3 cm) were observed. These measurements were combined with additional environmental variables (Table 1) to explain the regrowth patterns of vegetation on the forest floor. This was accomplished using correlation analysis (Pearson's *r*), simple regression (*R*<sup>2</sup>), multiple regression (*R*<sup>2</sup>, standardized regression coefficients  $\beta$ ), and distance-based redundancy analysis (db-RDA, *R*<sup>2</sup><sub>adj</sub>, triplots). All unstated *p* values were below 0.001.

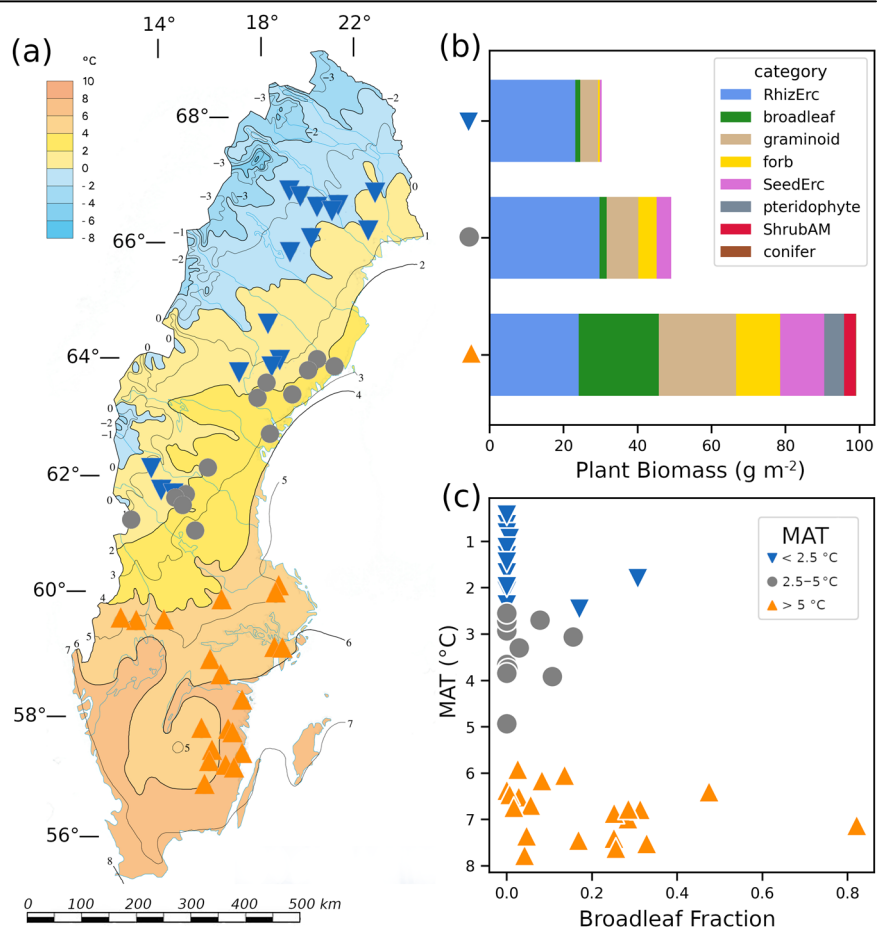
### Conifer-induced barriers to plant regrowth diversity can be reduced by wildfire burning

Of the sampled environmental variables, MAT provided the greatest explanation for the species richness of recovering plant communities across the 49 burn scars (*R*<sup>2</sup> = 0.594, Supplementary Fig. 1a). This relationship was further constrained (*R*<sup>2</sup> = 0.695, MAT  $\beta$  = 0.915, Fig. 3a, Supplementary Table 1) by the basal area of surviving conifer overstory (LiveConifer,  $\beta$  = -0.202) and the concentration of microbial biomass in the soil (MicConc,  $\beta$  = 0.337). The two general fungal phospholipid-derived fatty acid (PLFA) markers 18:1 $\omega$ 9 (*r* = -0.629) and 18:2 $\omega$ 6,9 (*r* = -0.596) were those most strongly negatively correlated to MAT. In contrast, all significant (*p* < 0.05) positive PLFA correlators with MAT were from gram-positive bacteria (i16:0, i17:0, 10Me16, 10Me17, and a17:0). High proportions of gram-positive to gram-negative bacteria (GP:GN) have been linked to oligotrophic processing of soil organic matter<sup>23</sup> and the biotic release of N to the soil solution within the current study's plots<sup>17</sup>. This means that wildfires can replace components of fungal communities with nutrient-mobilizing saprotrophic bacteria in proportions that are related to climate.

Under these conditions, LiveConifer failed to provide any restrictions on the mobilization of inorganic N to the soil solution (iN, *p* = 0.757) and did not significantly contribute to the differentiation of plant species or functional groups regrowing below the forest canopy in db-RDA (Fig. 4).

**Fig. 1 | Study site locations and vegetation survey.**

**a** The 49 separately sampled wildfires are shown on a map of mean annual temperature (MAT) over the normal period of 1961–1990 provided by the Swedish Meteorological and Hydrological Institute. **b** The plots were divided into three MAT ranges with eight plant functional group contributions to total subcanopy biomass plotted in bar charts. RhizErc: ericaceous species that tend to resprout from their rhizome after fire, broadleaf: broadleaved tree species, graminoid species, forb species, SeedErc: ericaceous species that tend to germinate from seed after fire, pteridophyte species, ShrubAM: arbuscular mycorrhizal shrubs, and conifer species. **c** Across the full range of sampled MAT, the percentage of broadleaf tree contribution to the recovering biomass was plotted. Upwards pointing orange triangles: forests with greater than 5 °C mean annual temperature, downwards blue triangles: less than 2.5 °C, and gray circles: forests in between these values.



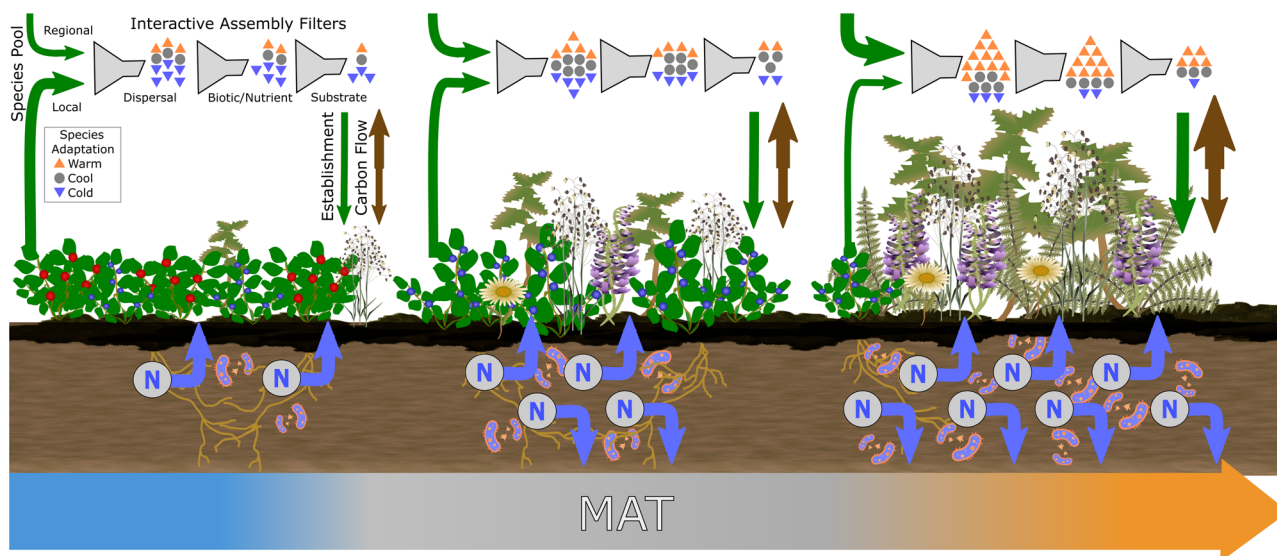


**Fig. 2 | Conceptual diagram illustrating how mean annual temperature may affect the interplay between species pools and different environmental filters during the establishment of plant communities after fire.** Previous observation in the current study’s plots found microbial communities to rapidly reassemble within the first year after fire, shifting fungal proportions to nutrient-mobilizing bacterial decomposers over increasing mean annual temperature (MAT)<sup>17</sup>. In order for primary production to outpace enhancement of decomposition in a warming climate, boreal forests need to either increase regrowth rates of previously occupant vegetation or transition to more warmth-adapted plant species. In the case of plant community turnover, novel species must pass through multiple environmental filters in order to contribute to forest biomass accumulation. It was hypothesized that shifts away from ericoid and ectomycorrhizal inhibition of plant diversity and nutrient cycling, under burning and increasing MAT, would allow for stronger

postfire establishment of more temperate vegetation structure, such as greater proportions of broadleaf trees in regrowth on the forest floor. Despite the relaxing of these bio-nutrient-associated filters at higher MAT, a combination of poor soil substrate quality (thick organic layers) and dispersal limitation (here unmeasured) was expected to continue to inhibit overall species richness of plant community assembly. These complex interactions were anticipated to emerge more simply as a biodiversity constraint on the ability of plant communities to utilize increasing MAT to acquire biomass across the 49 sampled plots. A potential consequence of these limitations is a mobilization of carbon and nutrient (N, downward arrows: leaching, upwards: biotic immobilization) away from the ecosystem at rates faster than their reaccumulation, potentially establishing plant priority effects that determine longer term trajectories of forest recovery and associated carbon storage capacity.

Furthermore, across all sampled plots, there was relatively little conifer regeneration on the forest floor (< 0.1% of total recovering biomass), despite more vigorous *Pinus sylvestris* recruitment previously observed during the first years after wildfire in boreal Eurasia (e.g., > 100,000 seedlings ha<sup>-1</sup><sup>24</sup>, two orders of magnitude higher than the current study’s estimate of about 1500 seedlings ha<sup>-1</sup> sampled over 47.2 m<sup>2</sup> of biomass cuttings). No conifer seedlings were found to reach above the understory, as visually surveyed across the 1.96 ha of the 49 plots. Seedlings below the understory are expected to have reduced survival rates due to competition with forest floor plants, including for light<sup>25,26</sup>.

These combined results demonstrate a wide range of fire severities capable of mitigating the capacity of the previously dominant conifer overstory to utilize ecosystem resources liberated after fire in order to recover, propagate and thereby influence the assembly patterns of competing vegetation in the early postfire environment. However, a residual influence of surviving trees was detected in their relationship to reduced species richness of regrowing plant communities. This limitation was potentially mediated by the replacement of conifer-supporting fungi with more opportunistic microbes capable of driving soil turnover conducive to a greater diversity of plant establishment.

The propagation of boreal conifers has been observed to require genetically specific ectomycorrhizal fungi to maximize generation success<sup>27,28</sup>. Once stressed, these microbes can require over a decade to recover<sup>29</sup>. A combination of drought, wildfire, and climatic maladaptation may have damaged mycorrhizal associations supportive of conifer resource acquisition and reproduction in the current plots. Prolonged study of the recovery capacity of boreal conifers is crucial to better determine their contributions to the forest C cycle at the decadal scale. However, the current study reveals an important window of time following wildfire burning, under current climatic conditions, where coniferous control over nutrient cycling can be breached even by low-severity wildfire<sup>17</sup>, opening boreal forests to plant community turnover and consequent shifts toward alternate ecosystem function. Notably, the reductions in fungal communities over gradients of MAT suggest globally-dispersed observations of poor conifer wildfire resilience<sup>15,16,30,31</sup> may be connected to reductions in sensitive mycorrhizal fungal communities under the influence of climatic warming.

**Table 1 | Independent variables used in regression and distance-based redundancy analyses**

Variable	Unit	Derivation
MAT	°C	1961–2017 averaged mean annual temperature
MAP	mm	1961–2017 averaged mean annual precipitation
LiveConifer	m <sup>2</sup> ha <sup>-1</sup>	Basal area of living conifers
ResOL	cm	Residual organic layer thickness in burnt plots
BurnDepth	cm	Estimated reduction of organic layer thickness due to fire
ρ	kg m <sup>-3</sup>	Organic layer bulk density
C:N	–	Organic layer total C divided by total N
pH	–	pH value extracted from the duff layer
iN	ppm	Resin capsule adsorbed NH <sub>4</sub> and NO <sub>3</sub> in organic soil
GP:GN	–	Ratio of gram-positive to gram-negative bacterial PLFA markers
MicConc	nmol g <sup>-1</sup>	Concentration of PLFA markers per duff sample mass

Variable names are given alongside their unit and a description of their formulation.

**Ericoid shrubs can provide a secondary resilience mechanism to forest state shifts**

Under the limited ability of surviving conifer overstory to control nutrient mobilization, the proportion of rhizomatously resprouting ericoid shrubs in

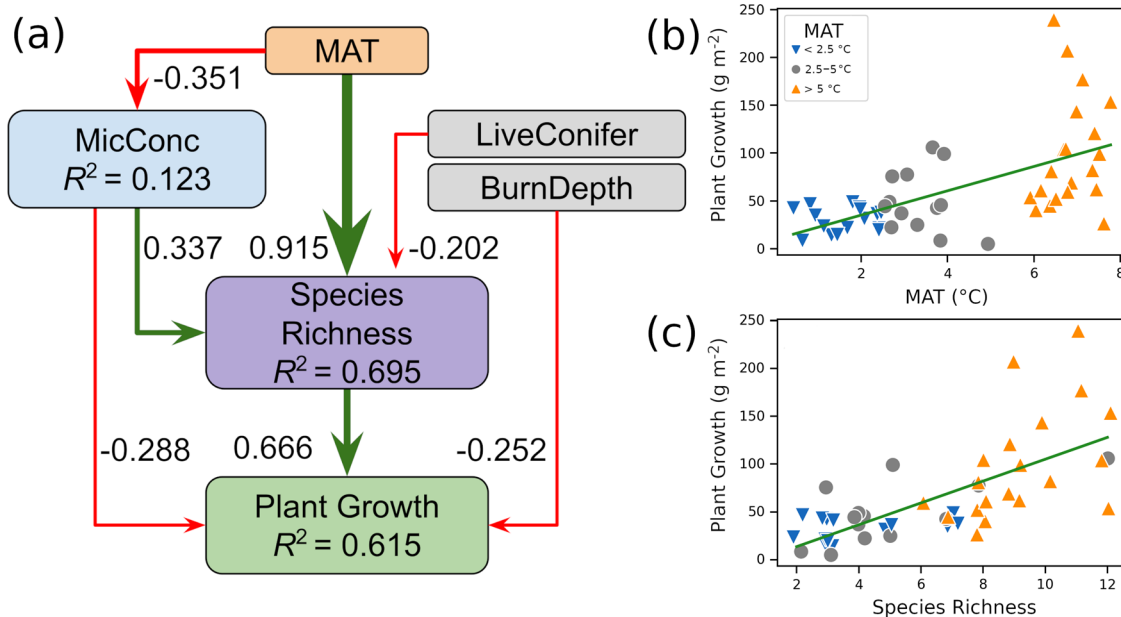


**Fig. 3 | Biodiversity mediation of temperature effects on plant growth.** **a** Two multiple regression results explaining species richness and plant growth were visualized with incoming arrows labeled, colored and sized according to standardized regressions coefficients of predictor variables. All significant regressions ( $p < 0.05$ ) between predictor variables are also presented accordingly. Simple regressions of biomass regrowth on MAT (**b**,  $R^2 = 0.353$ ) and species richness

(**c**,  $R^2 = 0.489$ ) were plotted. Heteroscedasticity of the MAT regression was reduced by shifting plot plant growth values across the species richness axis. A random number between  $\pm 0.2$  was added to the species richness values during chart generation to improve legibility. Upwards pointing orange triangles: forests with greater than  $5^{\circ}\text{C}$  mean annual temperature, downwards blue triangles: less than  $2.5^{\circ}\text{C}$ , and gray circles: forests in between these values.

the sampled regrowing vegetation (RhizErc) was negatively related to soil inorganic N availability (iN) and the nutrient-mobilizing GP:GN in db-RDA (Fig. 4b). RhizErc was also directly negatively related to GP:GN ( $r = -0.575$ , Supplementary Fig. 1b). Hence, ericoid mycorrhizas appeared to play an important role in the immobilization of forest N after burning. Furthermore, the apparent suppression of saprotrophic activity resembled the Gadgil effect studied in mature forests<sup>32</sup> but instead regarding the competition of ericoid mycorrhizas with bacterial decomposers in the postfire environment.

In undisturbed systems, ericoid mycorrhizas are known to be highly competitive in their ability to regulate the N cycle<sup>18</sup>. Despite their relatively small standing biomass compared to the overstory, ericaceous shrubs have a high material turnover and are therefore an important C source and nutrient sink to, and from, the soil and can even suppress tree seedling growth<sup>19,33</sup>. Ericoid mycorrhizal fungi can survive without plants during periods of disturbance allowing for a quick reestablishment of resource exchange with their resprouting host vegetation<sup>18</sup>. The ability of ericoid mycorrhizas to substitute the C-provisioning and nutrient immobilizing capacity of coniferous overstory presents an important and overlooked resilience mechanism of northern forests to climate driven deborealization (i.e., shifts from conifer- to broadleaf-dominated forest, with associated increases in rates of nutrient cycling and reduced soil organic layer depth).

Of the species associated with the variable RhizErc, *Vaccinium myrtillus* was most responsive to iN and the residual thickness of the organic layer (ResOL) in db-RDA. This species is important for C dynamics in Fennoscandian forests<sup>19,33</sup>, though functional genetic adaptation to broad ranges of climate may be compromised by the asexual sprouting mechanisms after fire when combined with local warming<sup>34</sup>. MAT related negatively to RhizErc ( $r = -0.688$ , Supplementary Fig. 1c) and positively to GP:GN ( $r = 0.531$ , Supplementary Fig. 1d), meaning boreal resilience provided by ericaceous understory against accelerated nutrient cycling supportive of broadleaf encroachment may dwindle under continued climatic change. High-severity wildfire that removes ericaceous rhizomes along with organic layer material may reduce barriers to the establishment of novel species, especially broadleaf trees. However, lower-severity wildfire combined with

forest warming may suppress important primary production and nutrient retention by ericoids, without promoting alternate growth. This could lead to the opening of extended resource drains from the ecosystem through the mineralization and mobilization of C and nutrient stored within the forest floor, potentially limiting future capacity to either recover previous forest structure or transition to broadleaf dominated forest<sup>17</sup>.

### Climate warming and wildfire can prime soils for broadleaf overstory growth

The documented fire-resilience of arbuscular mycorrhizal fungi<sup>29</sup>, and their ability to associate with a range of boreal-adapted broadleaves<sup>35</sup>, provides them an initial advantage in the postfire environment over slower-recovering, often host-specific, ectomycorrhizal fungi. The initial restructuring of belowground communities through the replacement of conifer-associated microbes with nutrient-mobilizing bacteria has the potential to prime soils for the establishment of more temperate, N-demanding plant species such as broadleaf overstory at the expense of the regeneration capacity of conifers.

Among the regrowing plant functional groups, broadleaf trees were most responsive to the combined effects of MAT and the nutrient-mobilizing GP:GN in db-RDA (Fig. 4b). The percentage of broadleaf biomass contribution to the recovering plant communities experienced a distinct boost from 3.9% to 20.4% above  $5^{\circ}\text{C}$  MAT (Fig. 1c). Much of this contribution in cooler regions (i.e., less than  $5^{\circ}\text{C}$  MAT) was derived from prefire occupant birch species (52.3% broadleaf biomass therein), though outlying broadleaf proportions were observed under the singular occurrence of the off-site derived *Salix sp.* (10.7% plot biomass, 17.1 cm ResOL) and *Sorbus aucuparia* (15.1% plot biomass, 8 cm ResOL). Broadleaf biomass was not related to ResOL in db-RDA, however. Residual organic layer thicknesses ranged from 2.5 to 17.1 cm (mean 7.0 cm), mostly well-above the 2 cm threshold below which explosive broadleaf growth in Sweden has been recorded at similar time-after-fire (averaging 17,000 seedlings  $\text{ha}^{-1}$ )<sup>36</sup>.

The results of the current study, when compared to previous observations of broadleaf growth dynamics under extreme fire conditions within the region<sup>36</sup>, exhibit a broad restrictive control of the

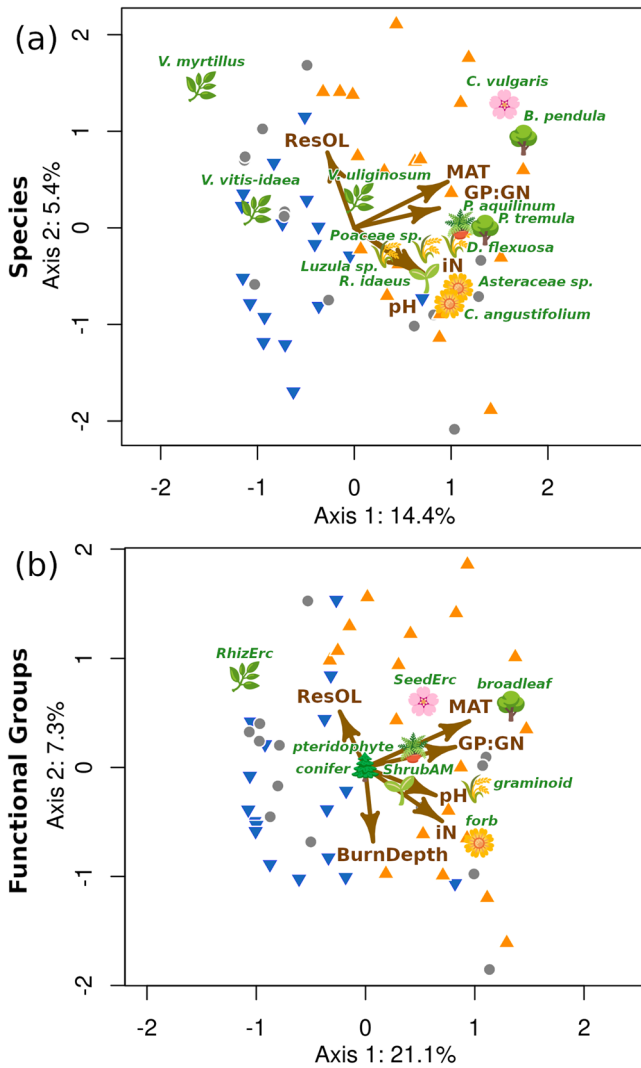


**Fig. 4 | Response of plant community development over environmental gradients.** Distance-based redundancy analysis explaining sampled plant species (a,  $R^2 = 0.300$ ,  $R^2_{adj} = 0.219$ ) and functional groups (b,  $R^2 = 0.427$ ,  $R^2_{adj} = 0.345$ ). All displayed axes are significant ( $p < 0.05$ ). Species scores in the upper panel were doubled to improve legibility. Upwards pointing orange triangles: forests with greater than 5 °C mean annual temperature, downwards blue triangles: less than 2.5 °C, and gray circles: forests in between these values. Results demonstrate a clear separation of resprouting boreal ericoids (RhizErc) from a greater diversity of vegetation by the sampled environmental variables.

residual organic soil layer on broadleaf tree propagation, with this restriction only partly overcome by the replacement of fungal communities with soil fertilizing bacteria under increased MAT. Although, specific locations provided outlying broadleaf tree growth even in cooler, less-fertile regions, implying establishment bottlenecks may have arisen from limited dispersal of broadleaf species in northern areas. The current climatic conditions across the boreal region may therefore be able to support a greater variety of plant species than what can be provisioned by landscapes both naturally and artificially organized under the conditions of the previous century. The ability of burnt forests to recapture C after fire appears to be determined by multiple, interacting controls derived from postfire soil conditions and regional variation in species pools under the influence of climate. As a consequence, the utilization of resources made available by wildfire burning may be bounded by restricted plant diversity under longer and warmer growing seasons associated with increased MAT.

### Carbon recapture can be limited by plant biodiversity

Of the environmental variables measured, MAT best explained plant biomass recovery rates on the forest floor ( $R^2 = 0.353$ , Fig. 3b). However, recovery rates under this relationship became increasingly variable at higher levels of MAT, with this variation better constrained when instead explained by species richness ( $R^2 = 0.489$ , Fig. 3c). When combining species richness with the environmental variables, the best model to explain biomass recovery ( $R^2 = 0.615$ , Fig. 3a, Supplementary Table 2) included the predictor variables species richness ( $\beta = 0.666$ ), MicConc ( $\beta = -0.288$ ) and BurnDepth ( $\beta = -0.252$ ).

These results suggest that macroclimatic influence on early postfire plant regrowth on the forest floor is largely mediated by species richness limitations during initial plant community assembly. The growth patterns discussed above suggest this limitation is driven by both the availability of plant generative material and site conditions conducive to their establishment. Furthermore, vegetation regrowth appears to be especially restricted under moderate fire severity which burns deep enough into the soil to alter plant and microbial regenerative structure, while leaving behind enough legacy material to inhibit novel species establishment. The current study provides a direct demonstration of the influence of plant biodiversity, as modulated by natural environmental interaction, on the ability of boreal forests to recapture C in the years immediately following wildfire.

Mesocosm growth experiments generally show a positive relationship between initial species richness and peak system biomass. Yet species richness has a variable relationship to biomass in natural late-successional communities, implying a filtering effect during community assembly that benefits from expanded selection within initial pools of species function<sup>37</sup>. This theory aligns with the current study’s observation of initial diversity constraints on the accumulation of biomass in the sampled burn scars. When paired with warmth-enhanced decomposition, this effect has the potential to both delay the transition of forests to states of net C recapture and establish recovery trajectories limiting its maximal accrual. Much more research is needed to connect early forest recovery patterns to longer term growth trajectories, especially under conditions of adaptive mismatch between climate and extant vegetation<sup>38</sup>. However, extending understanding of biodiversity from small-scale experimentation and observation in mature systems to the greater spatiotemporal scales of forest disturbance cycles is important for better determining the C storage capacity of the boreal region in the coming decades of climate change.

### Conclusions

Across the near-entire climatic extent of boreal Fennoscandia, a relatively weak early recovery of boreal conifers was observed under a wide range of burn severity, resulting in less than 0.1% coniferous biomass contribution to resprouting vegetation at 2 years post fire. The density of surviving coniferous overstorey placed no constraints on nutrient mobilization and did not influence the composition of plant communities on the forest floor. Yet these conifers did manage to place restrictions on overall plant diversity. Plant-soil feedbacks emerged through the resprouting of ericoid shrubs, which suppressed both nutrient-mobilizing saprotrophic bacterial communities and overall N availability. This understory-enforced suppression mechanism dwindled under increasing warmth across the sampled climate gradient, and was paired with an increase in the proportion of broadleaf contribution to the recovering plant communities. Though, in warmer regions, an increased variability of overall plant recovery rate was constrained by limitations on establishing plant species richness. This restriction was further enhanced by low microbial community biomass concentration and the depth of burning in the soil organic layer, though depth of burn did not surpass thresholds known within the region to provide for the most rapid broadleaf tree growth.

It is therefore proposed that boreal forests have intermediate ranges of fire severity that can reduce plant-soil feedbacks supportive of regrowth, but leave in place those that inhibit more diverse plant colonization. A dual limitation of previously occupant and novel species growth under warmth-

enhanced rates of soil decomposition can provide for net postfire emissions of C and eutrophication of surrounding systems that are likely to become more extreme under the coming decades of climatic change<sup>17,39</sup>. Land cover shifts associated with this wildfire driven reorganization of elements have the potential to further determine atmospheric energy balance by adjusting surface reflectivity<sup>40,41</sup>. Extended postfire vulnerability of boreal C stores is expected to be greatest in regions with high concentrations of fire-resisting vegetation, such as boreal Eurasia, with successional dynamics that may not be well-adapted for providing plant function capable of quick recovery under changing burn extremities<sup>42</sup>. The ineffectiveness of surrounding forest structure in providing a diversity of generative material that is successful in burn scars under altered fire and climate regimes has the potential to be further limited by phenotypically uniform forest management and low landscape gene conductivity that restricts the pace of plant species shifts with regional warming. The resulting greenhouse gas fluxes that occur in the years following burning may be overlooked by a sustained focus within fire research on quantifying initial emissions of high-severity wildfire burning. Further time-extended quantification of boreal wildfire-associated emissions across the full range of burn severity are likely to become increasingly important for understanding the contribution of forests to the land-atmosphere C balance under continued global change.

## Methods

### Plot selection and climate analysis

The current study provides a survey of vegetation regrowth patterns utilizing 49 of the 50 separate wildfires occurring during summer 2018 in Sweden which were part of previous published studies linking climate variation to fire severity, microbial community shifts and nutrient mobilization<sup>17,43–45</sup>. The northernmost of these 50 plots was not sampled in the current study due to post-fire salvage logging which destroyed the developing vegetation community. The original 50 burnt plots were selected to maximize spread across climate gradients within Sweden from a pool of 325 fires identified from the summer 2018 period that had perimeters manually mapped by the Swedish Forest Agency. Mapping was performed by drawing perimeters around burn scars delineated using Normalized Burn Ratio (NBR) values derived from Sentinel-2 bottom-of-atmosphere corrected bands 8 and 12. Close to the highest NBR pixel values in each separate burn scar, one 20 × 20 m<sup>2</sup> plot was established for field sampling. Elevation data for each plot was provided by the Swedish Mapping, Cadastral and Land Registration Authority from a 50 m resolution digital elevation model<sup>46</sup>. Slope was calculated from this data using the “slope” function within the ArcGIS software environment. All forest stands were located on minimally sloping land (less than 15° slope). Topo-edaphically evaluated soil moisture potential (TEM), which was considered a metric of soil drainage, was used to avoid wetland areas<sup>47</sup>. TEM was provided at 10 m resolution and given as integer values ranging from 0 to 240 (in order of increasing moisture potential) and was based on the Soil Topographic Wetness Index<sup>48</sup> in areas where soil type information was available and on the two topographic indices Depth to Water<sup>49</sup> and the Topographic Wetness Index<sup>50</sup> where soil information was unavailable. Further details and data sources are provided in ref. <sup>43</sup>.

Application of these site-selection filters resulted in plots with mean annual temperature (MAT) and precipitation (MAP), ranging from 0.43–7.77 °C and 539–772 mm, respectively, during the years 1961–2017, using regional climate data provided by the Swedish Meteorological and Hydrological Institute (SMHI). Under a given set of macroclimatic conditions, ecosystem structure can alter temperature in the subcanopy and soil which together may have a more direct effect than regional MAT on the sampled biotic and abiotic factors of the current study. Three recently produced maps of mean annual temperature in the subcanopy at 15 cm above the forest floor<sup>51</sup> and in the soil between 0–5 cm depth and 5–15 cm<sup>52</sup> had strong multicollinearity with regional MAT ( $p < 0.001$ , Pearson's  $r > 0.94$  for all) and therefore only the macroclimatic values were used in analysis. Frost free days were calculated as the count of days per year when the average air temperature was above 0 °C. For each year, growing degree

days were the sum of daily average air temperatures that were above a threshold of 5 °C, each subtracted by 5 °C. The 49 plot values averaged over 1961–2017 for these two metrics were highly correlated with their respective MAT values ( $p < 0.001$ , Pearson's  $r > 0.98$  for both), indicating that the MAT variable was a representative measure of the variation in thermal energy directly useful to plant growth.

### Initial vegetation mortality and fire impact field survey

During the first field visit in summer 2019 (1 year post fire), plot-wide tree mortality was measured as the percentage of stems with zero green needles in their respective canopies<sup>53</sup> for all standing or lying trees with their base inside the plot boundaries and diameter at 130 cm from its base greater than 5 cm. For all stems surveyed, species were also recorded and assessed for fire damage to determine the mode of heat propagation during fire. This allowed for the production of the variable LiveConifer, which is the total basal area of living conifer stems (m<sup>2</sup> ha<sup>-1</sup>). The 49 burnt plots were largely dominated by *Pinus sylvestris* (Scots pine) with the percentage of *Picea abies* (Norway spruce) stems between 25% and 50% in five plots, between 50% and 75% in three plots, and greater than 75% in two plots. Birch stems (*Betula pendula* and *Betula pubescens*) were less than 25% in 44 plots and between 25% and 50% in six plots, of which only one was spruce dominant. All plots showed some visible charring of tree boles, though only three plots had greater than 1% plot-wide canopy blackening (i.e., evidence of crown fire). The observed lack of charring in the canopy led to the assumption that the majority of the direct heating impact of fire was restricted to the lower tree boles and soil layers and an average consumption of 90% of estimated prefire understory biomass, as discussed further in ref. <sup>43</sup>.

### Soil sampling and measurement

Soil-based variables were measured in previous work<sup>17,43</sup> so their derivations are only briefly described in this section. During the first field visits in 2019, four organic layer soil samples were taken at each plot corner in accordance with ref. <sup>43</sup>. The samples were dried at 40 °C for 3 days with volume and dry weight recorded, producing values for bulk density ( $\rho$ ) in units of kg m<sup>-3</sup>. The samples were pulverized, packed in tin capsules and combusted in a Costech ECS 4010 elemental analyzer, equipped with a 2 m packed chromatographic column for gas separation, to produce values of C and N fraction by sample weight. Dividing total C by N gave values for organic layer C:N. The thickness of the organic layer was measured in millimeters at 20 separate points equally spaced across each plot diagonal<sup>54</sup> and averaged to produced values for the variable ResOL (residual organic layer). These organic layer depth values were subtracted from identically performed measurements in unburnt plots paired to each burnt plot to give values for BurnDepth. Plot-pair matching methodology and more detail regarding soil measurements are provided by ref. <sup>43</sup>.

Before drying, a fraction of the duff portion of the samples, which was the organic layer with surface pyrogenic and litter layers removed (i.e., duff is the conglomerate of the F (partially decomposed material) and H (humic material) layers in accordance with the Canadian system of soil classification<sup>55</sup>), was sieved to 4 mm and freeze dried to be used for analysis of PLFA and pH. For pH measurement, 1.0 g of soil was mixed with 20.0 mL of deionized water (resulting in an approximated 1:2.5 volume:volume dilution) and shaken vigorously for at least 1 min. The electrode was immersed in this solution for an additional 1 min, giving stable readings to two decimal places.

### Phospholipid-derived fatty acid analysis

Phospholipid-derived fatty acid (PLFA) analysis was performed on the freeze-dried soil samples by the Swedish University of Agricultural Sciences, Umeå, Sweden with the extraction and methanolysis of the soil PLFA following the method in ref. <sup>56</sup> as modified by ref. <sup>57</sup>. Resulting fatty acid methyl esters (FAME) were separated with gas chromatography giving calibrated measures of 24 individual FAME compounds as nmol per g soil sample. Total measured PLFA can be used as a metric of living soil microbial biomass due to its tendency not to persist as soil organic matter<sup>58–60</sup>. The

spectroscopically measured FAME concentrations were utilized as an estimate of relative microbial biomass per mass soil ( $\text{nmol g}^{-1}$ ) across the sampled plots and abbreviated as “MicConc”. Gram-positive bacteria consisted of 10Me16:0, 10Me17:0, 10Me18:0, i14:0, i15:0, a15:0, i16:0, i17:0, and a17:0 markers<sup>23,58,61</sup>. Gram-negative bacteria were the sum of cy17:0, cy19:0, 16:1 $\omega$ 7, 16:1 $\omega$ 9, 17:1 $\omega$ 8, and 18:1 $\omega$ 7<sup>23,58,61</sup>. The quotient of the summed mass of each of these two groups formed the indicator GP:GN for each plot. More detail on PLFA processing is provided in ref.<sup>17</sup>.

### Nutrient analysis

During the 2019 field campaign, 3 resin capsules (PST-1 ion-exchange capsules, Unibest, Walla Walla, Washington) per plot were buried equally-spaced at about 5 m from the plot center in the organic layer consistently at ~2 cm above its interface with the mineral layer below. There they acted to adsorb solvated ions effectively irreversibly, providing a time-integrated view of nutrient mobilization into the soil solution. 137 viable resin capsules were retrieved during a second field campaign ~1 year later, with the remaining missing or damaged. While in the field, the capsules were cleaned by shaking vigorously in a sealed vial with several applications of clean deionized water until applied water was clear and free from debris. Capsules were kept refrigerated each in individual plastic bags and then sent to a commercial laboratory for processing.

Resin capsule processing involved further cleaning with deionized water and then extraction of resin capsule adsorbates individually by rinsing with 2 N HCl at a rate of 1 mL  $\text{min}^{-1}$  for 50 min, resulting in volumetric 50 mL solutions of leachate. Each solution was separately analyzed for concentration of  $\text{NH}_4$  and  $\text{NO}_3$  and given in ppm ( $\text{mg L}^{-1}$  for mass of N atom alone).  $\text{NH}_4$  and  $\text{NO}_3$  concentrations were determined from aliquots of the extract solutions using flow injection analysis (FIA) and UV/VIS spectroscopy with an FIALab-2500 (FIALab Instruments, Seattle, Washington). Resulting ppm values were matrix matched by identical processing of separate resin capsules which were soaked in 3rd party manufactured standard solutions of common soil ions. This procedure was performed before every run of 25 samples and provided an analytical repeatability within  $\pm 0.5\%$ . The resulting 137 sets of ppm values were averaged per plot providing 49 values for each of the two chemical species, which were summed per plot to give total resin adsorbed inorganic N (iN).

### Floristics survey

A floristics survey was performed for each of the 49 plots in summer 2020 (2 years post fire) to capture the vegetation establishment stage<sup>62</sup>. Each plot was divided into quarters and a  $40 \times 40$  cm sampling quadrat was placed randomly into each area. All vegetation within the quadrat was clipped at the soil surface and stored. This procedure was performed again but with the plot split in two instead of four areas, resulting in a plot-wide conglomerated sample of six cuttings. One plot was sampled seven times, though all biomass values were divided by total sample area per plot to give units of  $\text{g m}^{-2}$ .

Each plot sample was dried for 3 days at 40 °C and dry weight recorded for use in analysis. For each of the 49 plots, the recorded species weights were divided into eight functional group categories including broadleaf (tree species only), conifer, pteridophyte, forb, and graminoid. Shrubs were split into three additional categories: ericaceous species that tend to resprout rhizomatously after fire (RhizErc, including *Vaccinium vitis-idaea*, *Vaccinium myrtillus*, and *Vaccinium uliginosum*)<sup>63,64</sup>, ericaceous species that tend to germinate from seed (SeedErc)<sup>65</sup>, and arbuscular mycorrhizal shrubs (ShrubAM). No moss or lichen biomass was found, with the forest floor below the regrowing plants being covered by a layer of char and some postfire additions of plant litter.

Random sampling of the relatively small areas covered by the quadrats had the potential to miss the measurement of plant species present in each of the larger  $20 \times 20$  m<sup>2</sup> plots. However, during postfire plant community assembly information about species that can contribute to possible community assemblages in a given burn scar can also be missing due to stochastic processes (e.g., absent from surrounding species pools or

succumbing to priority effects), thereby requiring regionally dispersed replication for improved statistical constraint on the drivers that influence development of plant community structure. The current study design chose to trade small sampled area per plot for spatially-dispersed, high replication across broad environmental gradients in order to reach this goal. As an added precaution, biomass to species richness relationships were derived from the same sampled area (within the quadrats), forming a directly measured relationship between these two properties. Furthermore, during methodological development, and at each of the 49 field sites, the  $20 \times 20$  m<sup>2</sup> plots were divided into 16 parts where a presence-absence plant survey was performed to assess plot heterogeneity. No alarming deviations in species occurrence relative to that sampled in quadrat cuttings were detected. Notably, across all plots, no prominent conifer seedlings were observed, which aligned with conifer biomass observations being restricted to only seven, less than 5 cm tall seedlings found within the biomass cuttings. Therefore, the sampling methodology was determined to be well-suited for study of regional variation in plant community response to wildfire and the implications for C cycling.

### Calculation of plant diversity and regrowth rate

Species richness was calculated simply as the number of plant species within biomass samples per plot. Regrowth rate of the sampled plant communities was calculated as the total dry biomass collected per burnt plot sampled area measured in summer 2020 and given in units of  $\text{g m}^{-2}$ .

### Correlation, simple regression and multiple regression model selection

Simple regression was performed using *scipy.stats.linregress* in Python 3 and provided significance via a *p* value and an additional calculation of bivariate correlation using Pearson's *r*. Multiple regression was performed by inputting standardized variables (i.e., converted to Z-scores) to the *OLS* class in the *statsmodels*<sup>66</sup> package using the Python 3 interpreter. The *OLS* class used the ordinary least squares regression approach to predict a single response variable based on linear combinations of predictor variables and gave as an output  $R^2$ ,  $R^2_{adj}$ , Akaike information criteria (AIC), and Bayesian information criteria (BIC) values for the model fit as well as standardized regression coefficients ( $\beta$ ) for the explanatory variables<sup>67</sup>. Multiple regression model selection was performed by beginning with the dependent variable producing the highest  $R^2_{adj}$  value and adding the variables, one at a time, that most increased this value. Corrected AIC (AICc) was calculated as

$$AICc = AIC + \frac{2k^2 + 2k}{n - k - 1}$$

where *k* is the number of model parameters and *n* is the sample size<sup>67</sup>.  $\Delta AICc$  and  $\Delta BIC$  values were produced from the difference of the current model from the lowest AICc and BIC in the entire model selection process, respectively.

### Distance-based redundancy analysis

Due to the partly stochastic nature of early ecosystem assembly, plant species abundances often do not form linear or unimodal responses over environmental gradients, prohibiting the use of many common linear models to directly constrain interspecific variation, as was the case with the current floristics data. This problem can be overcome by first statistically analyzing metrics of community similarity, rather than individual species' abundance. To give insight into the ability of the environmental variables to explain plant species and functional group variation, distance-based redundancy analysis (db-RDA) was used on the 49 individual plots<sup>68</sup>. This approach utilized the class *capscale* from the R package *vegan* to transform the area-normalized plant biomass data into principal coordinates using the Bray-Curtis dissimilarity which were then predicted through standard redundancy analysis by the normalized environmental variables<sup>69</sup>. The data transformation allowed for the varied response patterns of individual plant species or functional group variables (i.e., non-

linear, non-unimodal) to be predicted with robust estimates of model performance given through parameters such as  $R^2_{adj}$ . Site and predictor variable scores were plotted along the two strongest axes of explanation with the non-transformed plant data projected as points to demonstrate their relationship to their constrained principal coordinates. Model selection was performed using the *vegan* function *ordi2step* to select the specific set of explanatory variables, each with  $p < 0.05$ , that produced models with the highest  $R^2_{adj}$ .

### Data availability

All original data collected and prepared for this manuscript is fully available at the following repository: <https://doi.org/10.5281/zenodo.10017293>. All additional data used for analysis in this paper was taken directly from the following publications: <https://doi.org/10.3389/ffgc.2023.1136354>; <https://doi.org/10.5194/bg-19-2487-2022>.

Received: 13 November 2023; Accepted: 20 March 2024;

Published online: 16 April 2024

### References

- Baltzer, J. L. et al. Increasing fire and the decline of fire adapted black spruce in the boreal forest. *Proc. Natl Acad. Sci.* **118**, e2024872118 (2021).
- Mekonnen, Z. A., Riley, W. J., Randerson, J. T., Grant, R. F. & Rogers, B. M. Expansion of high-latitude deciduous forests driven by interactions between climate warming and fire. *Nat. Plants* **5**, 952–958 (2019).
- Solarik, K. A., Cazelles, K., Messier, C., Bergeron, Y. & Gravel, D. Priority effects will impede range shifts of temperate tree species into the boreal forest. *J. Ecol.* **108**, 1155–1173 (2020).
- Delavaux, C. S. et al. Mycorrhizal feedbacks influence global forest structure and diversity. *Commun. Biol.* **6**, 1066 (2023).
- Liang, M. et al. Soil fungal networks maintain local dominance of ectomycorrhizal trees. *Nat. Commun.* **11**, 2636 (2020).
- Kadowaki, K. et al. Mycorrhizal fungi mediate the direction and strength of plant-soil feedbacks differently between arbuscular mycorrhizal and ectomycorrhizal communities. *Commun. Biol.* **1**, 196 (2018).
- Näsholm, T. et al. Are ectomycorrhizal fungi alleviating or aggravating nitrogen limitation of tree growth in boreal forests? *New Phytol.* **198**, 214–221 (2013).
- Clemmensen, K. E. et al. Roots and associated fungi drive long-term carbon sequestration in boreal forest. *Science* **339**, 1615–1618 (2013).
- Averill, C., Turner, B. L. & Finzi, A. C. Mycorrhiza-mediated competition between plants and decomposers drives soil carbon storage. *Nature* **505**, 543–545 (2014).
- Greene, D. F. et al. The reduction of organic-layer depth by wildfire in the North American boreal forest and its effect on tree recruitment by seed. *Can. J. For. Res.* **37**, 1012–1023 (2007).
- Johnstone, J. F., Hollingsworth, T. N., Chapin III, F. S. & Mack, M. C. Changes in fire regime break the legacy lock on successional trajectories in Alaskan boreal forest. *Glob. Change Biol.* **16**, 1281–1295 (2010).
- Walker, X. et al. Shifts in ecological legacies support hysteresis of stand-type conversions in boreal forests. *Ecosystems* **26**, 1796–1805 (2023).
- Alexander, H. D., Mack, M. C., Goetz, S., Beck, P. S. A. & Belshe, E. F. Implications of increased deciduous cover on stand structure and aboveground carbon pools of Alaskan boreal forests. *Ecosphere* **3**, art45 (2012).
- Mack, M. C. et al. Carbon loss from boreal forest wildfires offset by increased dominance of deciduous trees. *Science* **372**, 280–283 (2021).
- Sun, Q. et al. Climate variability may delay post-fire recovery of boreal forest in southern Siberia, Russia. *Remote Sensing* **13** <https://www.mdpi.com/2072-4292/13/12/2247> (2021).
- Kukavskaya, E. A., Buryak, L. V., Shvetsov, E. G., Conard, S. G. & Kalenskaya, O. P. The impact of increasing fire frequency on forest transformations in southern Siberia. *For. Ecol. Manag.* **382**, 225–235 (2016).
- Eckdahl, J. A., Kristensen, J. A. & Metcalfe, D. B. Climate and forest properties explain wildfire impact on microbial community and nutrient mobilization in boreal soil. *Front. For. Glob. Chang.* **6** <https://www.frontiersin.org/articles/10.3389/ffgc.2023.1136354> (2023).
- Ward, E. B., Duguid, M. C., Kuebbing, S. E., Lendemer, J. C. & Bradford, M. A. The functional role of ericoid mycorrhizal plants and fungi on carbon and nitrogen dynamics in forests. *New Phytol.* **235**, 1701–1718 (2022).
- Nilsson, M.-C. & Wardle, D. A. Understory vegetation as a forest ecosystem driver: evidence from the northern Swedish boreal forest. *Front. Ecol. Environ.* **3**, 421–428 (2005).
- Pichon, N. A., Kaarlejärvi, E. & Eskelinen, A. Seed limitation interacts with biotic and abiotic factors to constrain novel species' impact on community biomass and richness. *Ecol. Lett.* **26**, 908–918 (2023).
- Day, N. J. et al. Material legacies and environmental constraints underlie fire resilience of a dominant boreal forest type. *Ecosystems* **26**, 473–490 (2023).
- Ueyama, M. et al. Carbon dioxide balance in early-successional forests after forest fires in interior Alaska. *Agric. For. Meteorol.* **275**, 196–207 (2019).
- Fanin, N. et al. The ratio of gram-positive to gram-negative bacterial plfa markers as an indicator of carbon availability in organic soils. *Soil Biol. Biochem.* **128**, 111–114 (2019).
- Kharuk, V. I. et al. Wildfires in the Siberian taiga. *Ambio* **50**, 1953–1974 (2021).
- Häggström, B., Gundale, M. J. & Nordin, A. Environmental controls on seedling establishment in a boreal forest: implications for scots pine regeneration in continuous cover forestry. *Eur. J. Forest Res.* **143**, 95–106 (2024).
- Jessen, M.-T. et al. Understory functional groups and fire history but not experimental warming drive tree seedling performance in unmanaged boreal forests. *Front. For. Glob. Chang.* **6** <https://www.frontiersin.org/articles/10.3389/ffgc.2023.1130532> (2023).
- Gehring, C. A., Sthultz, C. M., Flores-Rentería, L., Whipple, A. V. & Whitham, T. G. Tree genetics defines fungal partner communities that may confer drought tolerance. *Proc. Natl Acad. Sci.* **114**, 11169–11174 (2017).
- Ibáñez, T. S., Wardle, D. A., Gundale, M. J. & Nilsson, M.-C. Effects of soil abiotic and biotic factors on tree seedling regeneration following a boreal forest wildfire. *Ecosystems* **25**, 471–487 (2022).
- Treseder, K. K., Mack, M. C. & Cross, A. Relationships among fires, fungi, and soil dynamics in alaskan boreal forests. *Ecol. App.* **14**, 1826–1838 (2004).
- Haberstroh, S. et al. Central European 2018 hot drought shifts scots pine forest to its tipping point. *Plant Biol.* **24**, 1186–1197 (2022).
- Vilà-Cabrera, A., Rodrigo, A., Martí-nez-Vilalta, J. & Retana, J. Lack of regeneration and climatic vulnerability to fire of scots pine may induce vegetation shifts at the southern edge of its distribution. *J. Biogeogr.* **39**, 488–496 (2012).
- Fernandez, C. W. & Kennedy, P. G. Revisiting the 'gadgil effect': do interguild fungal interactions control carbon cycling in forest soils? *New Phytol.* **209**, 1382–1394 (2016).
- Hensgens, G. et al. The role of the understory in litter doc and nutrient leaching in boreal forests. *Biogeochemistry* **149**, 87–103 (2020).
- Taulavuori, K., Laine, K., Taulavuori, E., Pakonen, T. & Saari, E. Accelerated dehardening in bilberry (*Vaccinium myrtillus* L.) induced by a small elevation in air temperature. *Environ. Pollut.* **98**, 91–95 (1997).



35. Karst, J. et al. Assessing the dual-mycorrhizal status of a widespread tree species as a model for studies on stand biogeochemistry. *Mycorrhiza* **31**, 313–324 (2021).
36. Gustafsson, L. et al. Rapid ecological response and intensified knowledge accumulation following a north European mega-fire. *Scand. J. For. Res.* **34**, 234–253 (2019).
37. Hagan, J. G., Vanschoenwinkel, B. & Gamfeldt, L. We should not necessarily expect positive relationships between biodiversity and ecosystem functioning in observational field data. *Ecology Letters* **24**, 2537–2548 (2021).
38. Reich, P. B. et al. Even modest climate change may lead to major transitions in boreal forests. *Nature* **608**, 540–545 (2022).
39. Granath, G. et al. The impact of wildfire on biogeochemical fluxes and water quality in boreal catchments. *Biogeosciences* **18**, 3243–3261 (2021).
40. Betts, R. A. Offset of the potential carbon sink from boreal forestation by decreases in surface albedo. *Nature* **408**, 187–190 (2000).
41. Ollinger, S. V. et al. Canopy nitrogen, carbon assimilation, and albedo in temperate and boreal forests: Functional relations and potential climate feedbacks. *Proc. Natl Acad. Sci.* **105**, 19336–19341 (2008).
42. Rogers, B. M., Soja, A. J., Goulden, M. L. & Randerson, J. T. Influence of tree species on continental differences in boreal fires and climate feedbacks. *Nat. Geosci.* **8**, 228–234 (2015).
43. Eckdahl, J. A., Kristensen, J. A. & Metcalfe, D. B. Climatic variation drives loss and restructuring of carbon and nitrogen in boreal forest wildfire. *Biogeosciences* **19**, 2487–2506 (2022).
44. Eckdahl, J. A., Rodriguez, P. C., Kristensen, J. A., Metcalfe, D. B. & Ljung, K. Mineral soils are an important intermediate storage pool of black carbon in fennoscandian boreal forests. *Glob. Biogeochem. Cycles* **36**, e2022GB007489 (2022).
45. Eckdahl, J. *Boreal Forest Wildfire in a Changing Climate*. Ph.D. Thesis (Dept of Physical Geography and Ecosystem Science, 2023).
46. Lantmateriet. Markhöjdmmodell nedladdning, grid 50+. <https://www.lantmateriet.se/sv/Kartor-och-geografisk-information/geodataprodukter/produktlista/markhojdmmodell-nedladdning-grid-50/#steg=1> (2021).
47. Naturvårdsverket. Markfuktighetsindex producerat som del av nationella marktäckedata, nmd 2018. <https://metadatakatalogen.naturvardsverket.se/metadatakatalogen/GetMetaDataByld?id=cae71f45-b463-447f-804f-2847869b19b0>.
48. Buchanan, B. P. et al. Evaluating topographic wetness indices across central New York agricultural landscapes. *Hydrol. Earth Syst. Sci.* **18**, 3279–3299 (2014).
49. Murphy, P. N., Ogilvie, J., Connor, K. & Arp, P. A. Mapping wetlands: a comparison of two different approaches for new brunswick, canada. *Wetlands* **27**, 846–854 (2007).
50. Beven, K. J. & Kirkby, M. J. A physically based, variable contributing area model of basin hydrology. *Hydrol. Sci. Bull.* **24**, 43–69 (1979).
51. Haesen, S. et al. Foresttemp - sub-canopy microclimate temperatures of European forests. *Glob. Change Biol.* **27**, 6307–6319 (2021).
52. Lembrechts, J. J. et al. Global maps of soil temperature. *Glob. Change Biol.* **28**, 3110–3144 (2022).
53. Sidoroff, K., Kuuluvainen, T., Tanskanen, H. & Vanha-Majamaa, I. Tree mortality after low-intensity prescribed fires in managed pinus sylvestris stands in southern Finland. *Scand. J. For. Res.* **22**, 2–12 (2007).
54. Kristensen, T., Ohlson, M., Bolstad, P. & Nagy, Z. Spatial variability of organic layer thickness and carbon stocks in mature boreal forest stands—implications and suggestions for sampling designs. *Environ. Monit. Assessment* **187**, 1–19 (2015).
55. Canadian Agricultural Services Coordinating Committee. *The Canadian System of Soil Classification* (NRC Research Press, 1998).
56. Bligh, E. G. & Dyer, W. J. A rapid method of total lipid extraction and purification. *Can. J. Biochem. Physiol.* **37**, 911–917 (1959).
57. White, D., Davis, W., Nickels, J., King, J. & Bobbie, R. Determination of the sedimentary microbial biomass by extractable lipid phosphate. *Oecologia* **40**, 51–62 (1979).
58. Joergensen, R. G. Phospholipid fatty acids in soil—drawbacks and future prospects. *Biol. Fertil. Soils* **58**, 1–6 (2022).
59. Zhang, Y. et al. High turnover rate of free phospholipids in soil confirms the classic hypothesis of plfa methodology. *Soil Biol. Biochem.* **135**, 323–330 (2019).
60. Frostegård, Å, Tunlid, A. & Bååth, E. Use and misuse of plfa measurements in soils. *Soil Biol. Biochem.* **43**, 1621–1625 (2011).
61. Willers, C., Jansen van Rensburg, P. & Claassens, S. Phospholipid fatty acid profiling of microbial communities—a review of interpretations and recent applications. *J. Appl. Microbiol.* **119**, 1207–1218 (2015).
62. Bartels, S. F., Chen, H. Y., Wulder, M. A. & White, J. C. Trends in post-disturbance recovery rates of Canada’s forests following wildfire and harvest. *For. Ecol. Manag.* **361**, 194–207 (2016).
63. Schimmel, J. & Granstrom, A. Fire severity and vegetation response in the boreal Swedish forest. *Ecology* **77**, 1436–1450 (1996).
64. Zyryanova, O. A., Abaimov, A. P., Bugaenko, T. N. & Bugaenko, N. N. Recovery of Forest Vegetation After Fire Disturbance, 83–96 (Springer Netherlands, Dordrecht, 2010). [https://doi.org/10.1007/978-1-4020-9693-8\\_5](https://doi.org/10.1007/978-1-4020-9693-8_5).
65. Granström, A. & Schimmel, J. Heat effects on seeds and rhizomes of a selection of boreal forest plants and potential reaction to fire. *Oecologia* **94**, 307–313 (1993).
66. Seabold, S. & Perktold, J. Statsmodels: econometric and statistical modeling with python. In *Proc. 9th Python in Science Conference* (2010).
67. Burnham, K. P. & Anderson, D. R. Multimodel inference: understanding aic and bic in model selection. *Sociol. Methods Res.* **33**, 261–304 (2004).
68. Legendre, P. & Anderson, M. J. Distance-based redundancy analysis: Testing multispecies responses in multifactorial ecological experiments. *Ecol. Monogr.* **69**, 1–24 (1999).
69. Oksanen, J. et al. *vegan: Community Ecology Package* (2022). <https://CRAN.R-project.org/package=vegan>. R package version 2.6-4.

## Acknowledgements

J.E. was supported by the strategic research area Biodiversity and Ecosystems in a Changing Climate, BECC, at Lund University. J.K. was supported by the Carlsberg Foundation (grant CF20-0238). D.M. was supported by funding from the European Research Council under the European Union’s Horizon 2020 research and innovation program (ECOHERB; grant no. 682707). Thank you to Rieke Lo Madsen and Femke Pijcke for vital contributions to the floristics survey. Field assistance from Caroline Hall, Mathias Welp, Neija Elvekjær, Geerte Fälthammar-de Jong, Lotte Wendt, Julia Iwan, and Henni Yläne was greatly appreciated. Thank you Tamara van Steijn for assistance with graphics generation. Natascha Kijun, Margarida Soares and Md. Rafikul Islam provided helpful feedback throughout the development of the manuscript. Thanks Julia Kelly for thoughtful suggestions regarding data analysis and interpretation. Two reviewers are appreciated for providing important insight and attentive suggestions that helped refine the manuscript.

## Author contributions

J.E.: conceptualization, data curation, formal analysis, investigation, methodology, resources, software, validation, visualization, writing—original draft preparation. J.K. and D.M.: funding acquisition and resources. J.E., J.K., and D.M.: project administration, supervision, writing—review and editing. All authors contributed to the article and approved the submitted version.

## Funding

Open access funding provided by Lund University.

### Competing interests

The authors declare no competing interests.

### Additional information

**Supplementary information** The online version contains supplementary material available at

<https://doi.org/10.1038/s43247-024-01333-7>.

**Correspondence** and requests for materials should be addressed to Johan A. Eckdahl.

**Peer review information** *Communications Earth & Environment* thanks Jill F. Johnstone and the other, anonymous, reviewer(s) for their contribution to the peer review of this work. Primary Handling Editors: Erika Buscardo and Aliénor Lavergne. A peer review file is available.

**Reprints and permissions information** is available at <http://www.nature.com/reprints>

**Publisher's note** Springer Nature remains neutral with regard to jurisdictional claims in published maps and institutional affiliations.

**Open Access** This article is licensed under a Creative Commons Attribution 4.0 International License, which permits use, sharing, adaptation, distribution and reproduction in any medium or format, as long as you give appropriate credit to the original author(s) and the source, provide a link to the Creative Commons licence, and indicate if changes were made. The images or other third party material in this article are included in the article's Creative Commons licence, unless indicated otherwise in a credit line to the material. If material is not included in the article's Creative Commons licence and your intended use is not permitted by statutory regulation or exceeds the permitted use, you will need to obtain permission directly from the copyright holder. To view a copy of this licence, visit <http://creativecommons.org/licenses/by/4.0/>.

© The Author(s) 2024